

V Riccardo, J R Last, A S Kaye

Classical and Fracture Mechanics Analysis of the Tails of the JET TF Coils

“This document is intended for publication in the open literature. It is made available on the understanding that it may not be further circulated and extracts or references may not be published prior to publication of the original when applicable, or without the consent of the Publications Officer, EFDA, Culham Science Centre, Abingdon, Oxon, OX14 3DB, UK.”

“Enquiries about Copyright and reproduction should be addressed to the Publications Officer, EFDA, Culham Science Centre, Abingdon, Oxon, OX14 3DB, UK.”

Classical and Fracture Mechanics Analysis of the Tails of the JET TF Coils

V Riccardo, J R Last, A S Kaye

EURATOM/UKAEA Fusion Association, Culham Science Centre,
Abingdon, Oxfordshire, OX14 3DB, UK.

ABSTRACT

The JET toroidal field (TF) coils are made of two 12-turn copper pancakes. The tails are designed to strengthen the inter-pancake joint and to transfer the tension between the tail and the bulk of the coil through shear in the inter-turn insulation.

Stresses in the tail region, due to the combination of thermal and mechanical loads, have been found to be close to the measured material strength. In the high tensile stress region at the truncated tip of the tail, the computed tensile strain release energy is close to the critical value typical for glass-fibre/epoxy insulation. In contrast, the computed strain release energy for a crack extending to the region of the peak shear stress is smaller than the critical shear strain release energy measured on specimens taken from a used coil. This indicates that even if a crack opens at the tail tip, it would propagate slowly, if at all.

1. INTRODUCTION

In operation the copper conductors of the JET toroidal field (TF) coils are subject to tensile hoop stresses. A stress concentration arises at the ends of the coil windings where special termination features, often referred to as tails (Fig.1), are located to strengthen the coil, both at the inter-pancake joints and at the current feed points.

Stresses in the tail region are due to the thermal and tension gradients between the active conductors and the tail, where no current flows and hence no hoop load or power dissipation are present. The tails are tapered along their length and most of the tensile stress is gradually transferred via a constant shear stress in the inter-turn insulation. However, the tail tip is truncated whilst the insulation thickness remains constant, producing local peaked shear stresses near the tip. If there was no tail

(i.e. sudden truncation of the conductor), the peak shear stress would be larger. On the other hand, if the insulation thickness increased while the conductor tapers, the peak shear stress

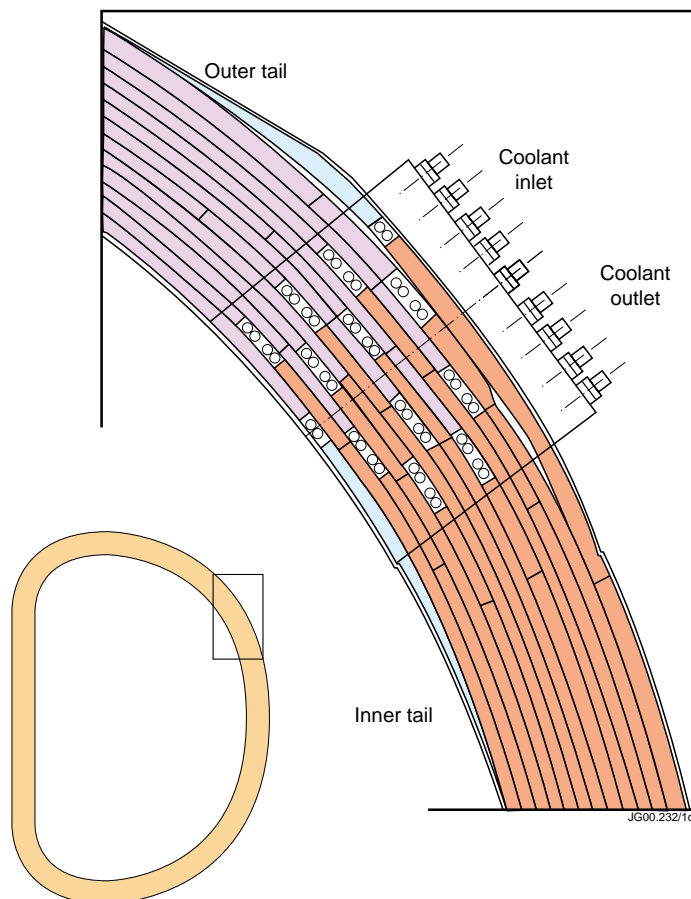


Fig.1: Coil transition region showing the position of coolant connections, brazed joints and tapered tails (darker greys for warmer copper)

could be reduced. High tensile stresses also occur at the tail tip, and these are less dependent on the tail and insulation geometry.

Both shear (Fig.2) and tensile (Fig.3) stresses approach the measured material strength [1,2], so cracks may form in these regions; this paper assesses the growth rate of such cracks.

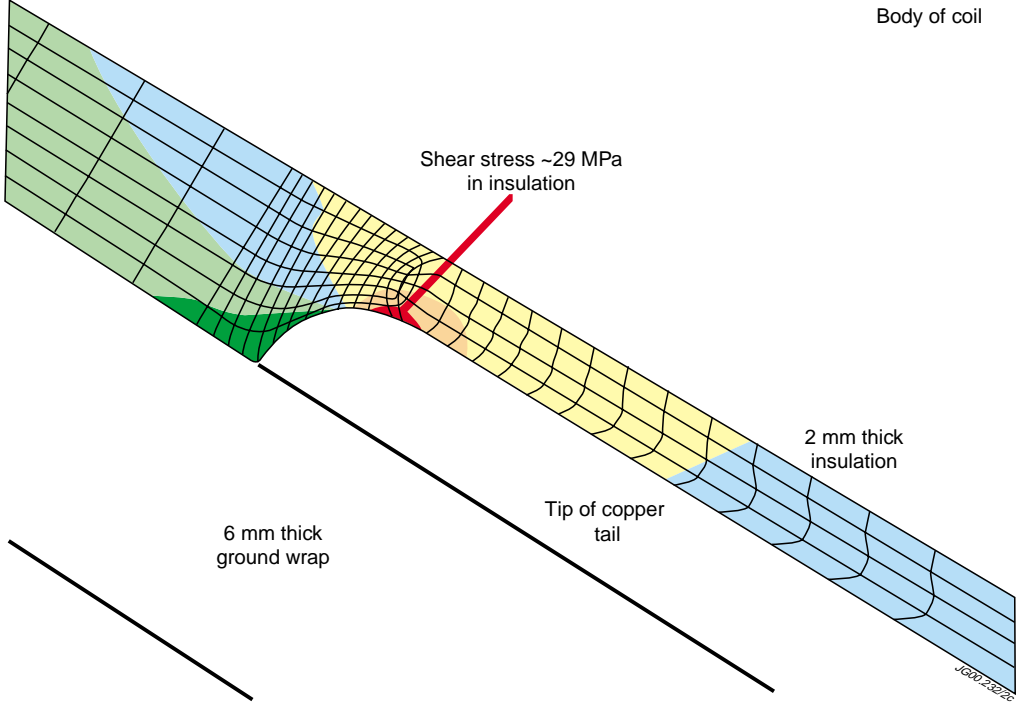


Fig.2: Shear stress in the insulation at the tip of the tail

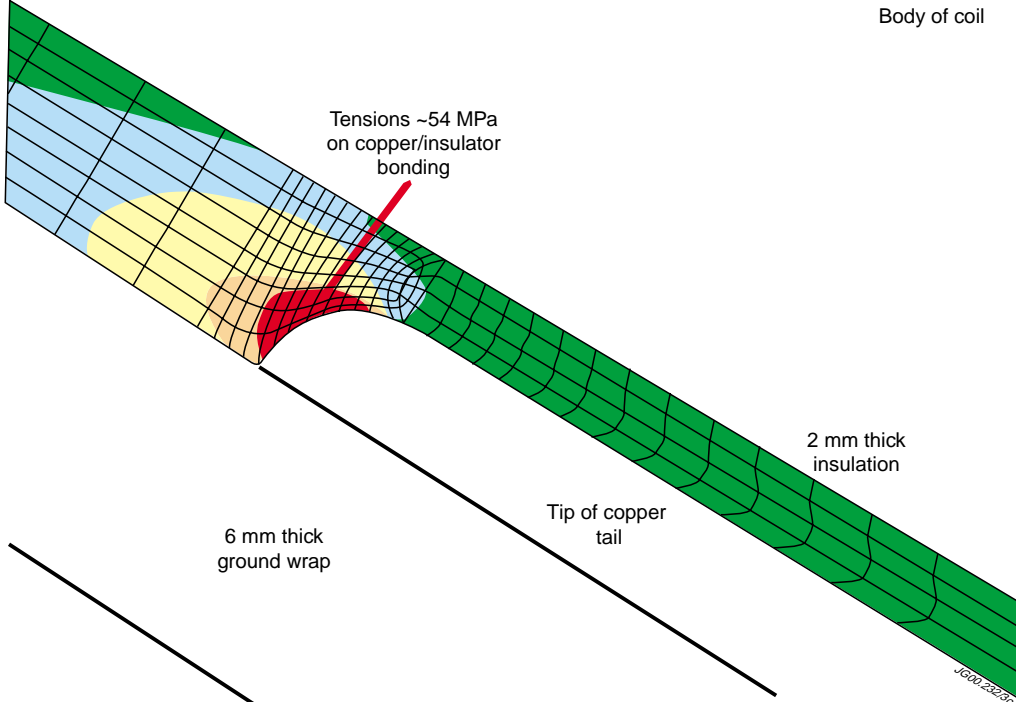


Fig.3: Tensile stress in the insulation at the copper/insulation bonding at the tail end face

2. NON-LINEAR INSULATION RESPONSE

Fatigue shear tests using Iosipescu samples showed that cyclic creep occurs in the insulation. This could allow stress peaks calculated with elastic properties to relax [3]. The data collected in the fatigue tests has been used to calibrate the plastic material properties of the insulation (Fig.4). With these insulation properties and at full TF current (77.8 kA) and pulse length ($I^2t=112 \cdot 10^9 \text{ A}^2\text{s}$), the peak shear stress decrease from 29 MPa to 27 MPa and the peak tensile stress from 54 MPa to 43 MPa. In operation the pulse length at high field is limited to $90 \cdot 10^9 \text{ A}^2\text{s}$, which reduces the peak stresses by a further 10%. In addition, the shear stress values quoted here are for a 2 mm thick insulation at the tip of the tail. Manufacture drawings show the insulation tapering from 2 mm to 3 mm along the last ~100 mm of the tail and the samples extracted from one transition piece have 2.5 mm of insulation at ~25 mm from the tip [1]. Therefore the actual peak shear stress may be lower as the peak shear stress varies as the inverse of the square root of the insulation thickness.

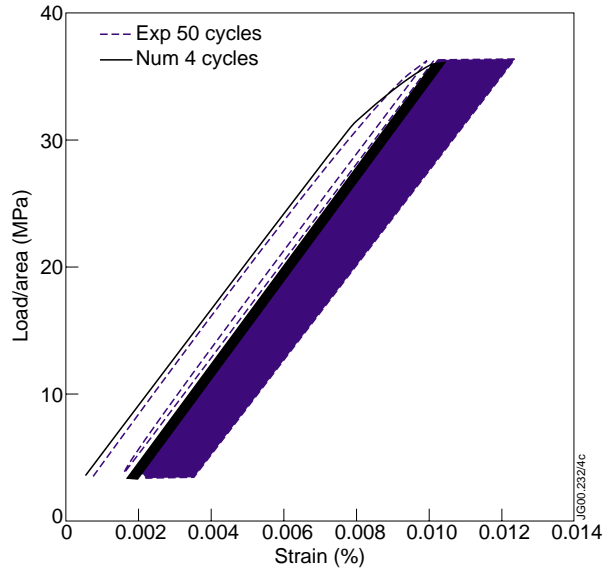


Fig.4: First 50 cycles of a typical cyclic shear test (failed after 225 cycles) and results of the FE simulation.

3. STRAIN RELEASE ENERGY ALONG THE CRACK PATH

For analytical studies, cracks have been assumed to initiate in the high tensile stress region (Fig.3). Here the computed strain release energy (~200 N/m, Fig.5) is close to typical critical mode I (tension) strain release energy, J_{Ic} , for insulation as used in the JET TF coils (tests to measure the actual J_{Ic} are in progress). For each crack length at which the strain release energy has to be computed, an FE model was developed (by modifying a bas 2D model of the transition region) in order to include the tip support, which has a singularity. Seven crack lengths (Fig.6), in the range 1 to 7 mm, have been analysed to show that in the high shear region the computed strain release energy is <400 N/m in all cases (Fig.5), even when the

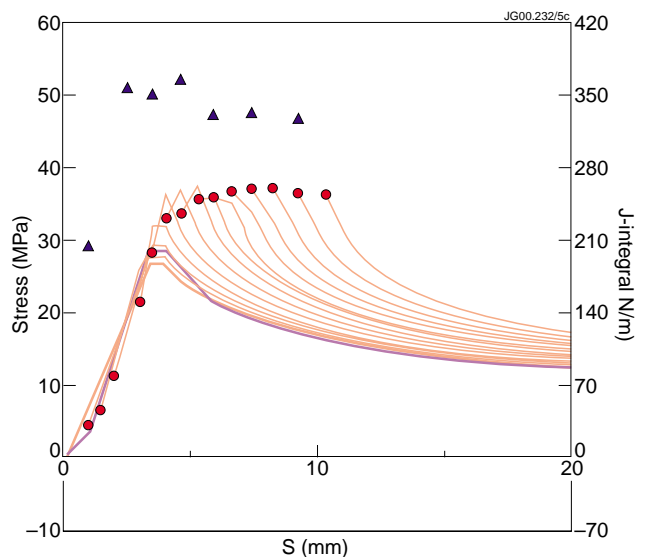


Fig.5: Computed shear stress (left axis) and strain release energy (triangles, right axis) along the assumed path of the delamination at the tip of the tail (s in Fig. 6). The full dots are at the location of the first bonded element.

peak shear stress increases significantly (from 27 MPa to 37 MPa). The critical mode II (shear) strain release energy, J_{IIc} , measured on specimens taken from a used TF coil (see Sect. 4) is at least 3 times larger than the computed strain release energy. It is therefore anticipated [4] that even if the tensile stresses initiate a crack, this would subsequently propagate slowly, if at all, in mode II. In fact (see below), the load equivalent to 400 N/m is 56% of the measured critical load, where no crack growth could be measured. The measured growth rate remains less than 10^{-6} m/cycle at 75% of the critical load (i.e. less than 1 mm in 1,000 cycles).

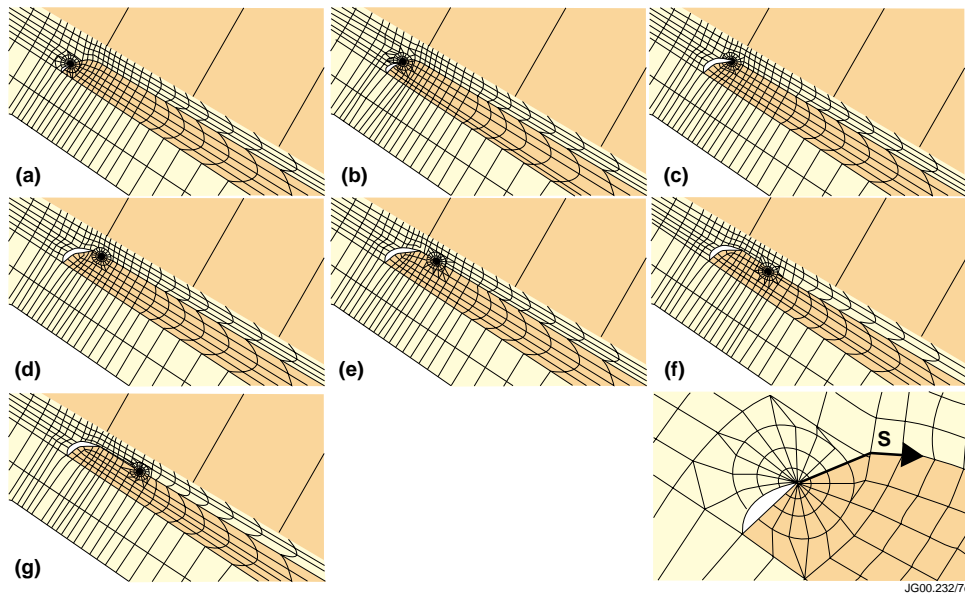


Fig.6: FE models (A-G) used to compute the strain release energy: zoom on a $45 \times 30 \text{ mm}^2$ region of the model where the typical element size in the copper tail and in the inter-turn insulation is 0.5 mm.

4. PROGRESS IN THE MEASUREMENT OF CRACK PROPAGATION

The critical strain release energy has been measured on specimens (copper/insulation/copper sandwiches) taken from the inter-turn region of a slice of TF coil and subjected to ENF (End Notched Flexure [5]) tests. The resulting critical mode II strain release energy has been found to be $1250 \pm 130 \text{ N/m}$.

Attempts to measure the cyclic crack growth rate have been done on two sets of 6 ENF samples. Specimens which had the pre-crack opened with a blade usually showed some growth in the first few hundred cycles (probably due to settling of the crack). After that most of the specimens did not show any growth of the main crack for up to 250,000 cycles and for loads up to 70% of the critical load. The unbroken specimens developed additional parallel 10÷15 mm long cracks at the end where the pre-crack had been introduced. One specimen, cycled at 70% of the critical load, showed no additional cracks and broke in a static-like manner after ~8,000 cycles. More data has been collected from the specimens which had the pre-crack opened with a purpose-made tool. In one specimen, cycled at 75% of the critical load, the crack grew as in a creep test (fast initial growth followed by a long period of very slow creeping growth, rapidly

increasing towards the end). Three specimens did not show any crack growth when cycled at 25%, 50% and 75% of the critical load, but had stable growth at 90% of the critical load (surviving 700, 2,000 and in excess of 20,000 cycles). The data collected from three of the tests is shown in Fig.7.

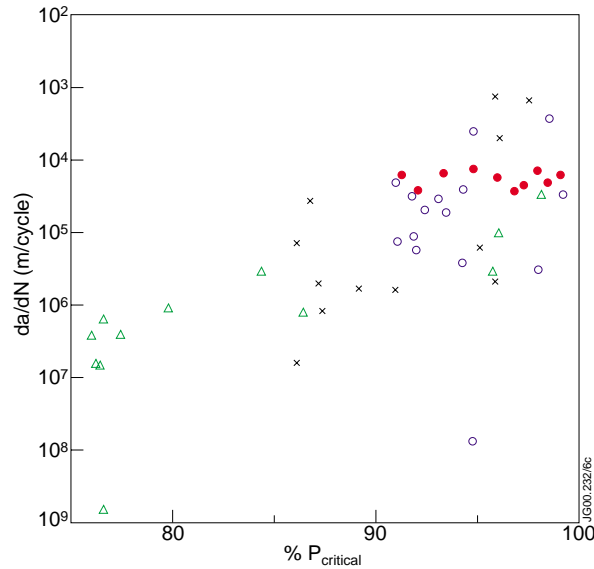


Fig.7: Crack growth rate versus % of critical load:

- △ microscope measurements on the specimen which survived 18,000 cycles at 75%;
- × compliance analysis of the last 2,000 of the specimen which survived 18,000 cycles at 75%;
- compliance analysis of the specimen which survived 2,000 cycles at 90%;
- compliance analysis of the specimen which survived 700 cycles at 90%.

5. DISCUSSION AND CONCLUSION

While the analytic work on the tails of the TF coils started during the 4 T Upgrade study has been completed, the experimental work is still under way.

The main aim of the present tests is to quantify the mode II crack growth rate in the insulation. The insulation in the sandwich specimens contained a double layer of pre-impregnated cloth, with localised micro-voids at the centre line and their results give an upper limit to the crack growth rate. The ground wrap insulation does not contain pre-impregnated cloth. Insulation-only specimens taken from the ground wrap will also be tested and will give a lower limit to the crack growth rate. The tail insulation has no pre-impregnated cloth either, and its weak feature, the copper/insulation bonding, has been proven to be stronger than the midplane pre-preg layer as most of the samples (5 out of 6) cracked there. There are no tail samples available for testing.

Presently operation at full TF current is limited to $<90 \cdot 10^9 \text{ A}^2 \text{ s}$ pulses ($\sim 3 \text{ s}$ TF flat top). If we assume a 5 mm crack, this corresponds to a strain release energy of $<300 \text{ N/m}$, which is less than a quarter of the measured critical value and gives rise to negligible crack growth. Operation at full field and $I^2 t$ (6.5 s TF flat top) gives rise to a stress field corresponding to 56% of the critical load. The corresponding crack growth is less than 1 mm in 1,000 pulses. JET has

cumulatively run the equivalent of ~150 pulses at full TF performance in its life, including ~200 pulses at >3.4 T.

A better understanding of the insulation and bonding characteristics will enlarge the safety margin of the TF coil tails and allow an increase in the pulse length at full field.

ACKNOWLEDGEMENTS

This work was performed partly in the framework of the JET Joint Undertaking and partly under the European Fusion Development Agreement (EFDA). The latter part was funded under the JET Operating Contract by EFDA.

The authors wish to thank J. Jeskins (JET), R. Mera and W.R. Broughton (NPL), and the members of the 4T-JSC-RAG.

REFERENCES

- [1] A. Kaye et al., The Reliability Assessment of JET Operation at a Toroidal Field of 4.0 T, SOFE18, 22-26 October 1999, Albuquerque.
- [2] P. Miele et al., Analysis and Tests of the TF magnet Insulation Samples for the JET Upgrade to 4 T, MT16, 27 September- 1 October 1999, Tallahassee.
- [3] C.T. Herakovich, Mechanics of Fibrous Composites, J. Wiley & Sons, New York, 1998, pp. 223-227 and 342-359.
- [4] T.L. Anderson, Fracture Mechanics, CRC Press, London, 1995, pp. 517-520.
- [5] W.R. Broughton, VAMAS Round Robin Project on Polymer Composite Delamination in mode I and mode II: Cyclic loading, NPL report DMM(A)47, March 1992.